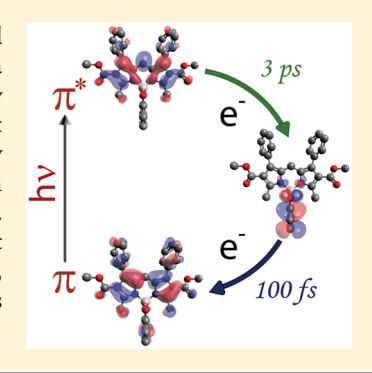


Rapid Excited-State Deactivation of BODIPY Derivatives by a Boron-**Bound Catechol**

Rachel K. Swedin, [†] Yuriy V. Zatsikha, [‡] Andrew T. Healy, [†] Natalia O. Didukh, [‡] Tanner S. Blesener, [‡] Mahtab Fathi-Rasekh, [§] Tianyi Wang, [‡] Alex J. King, [§] Victor N. Nemykin, **, [‡] and David A. Blank*, [†]

Supporting Information

ABSTRACT: The excited-state dynamics and energetics of a series of BODIPY-derived chromophores bound to a catechol at the boron position were investigated with a combination of static and time-resolved spectroscopy, electrochemistry, and density functional theory calculations. Compared with the difluoro-BODIPY-derived parent compounds, the addition of the catechol at the boron reduced the excited-state lifetime by three orders of magnitude. Deactivation of the excited state proceeded through an intermediate charge-transfer state accessed from the initial optically excited π^* state in <1 ps. Despite differences in the structures of the BODIPY derivatives and absorption maxima that spanned the visible portion of the spectrum, all compounds exhibited the same, rapid, excited-state deactivation mechanism, suggesting the generality of the observed dynamics within this class of compounds.



odular construction of molecular systems designed to translate the energy of absorbed light into the potential energy of charge separation has received considerable attention.^{1,2} Typical covalent constructs consist of three core components: a chromophore to absorb the light that also acts as an excited-state oxidant or reductant, an electron-donating or -accepting partner, and the molecular bridge between them. Chromophores based on the modification of a BODIPY core can provide strong light absorption, good stability under photolytic conditions, and broadly tunable absorption and redox properties.^{3,4} Substitution chemistry replacing the fluorines on the boron with a catechol, as illustrated at the top of Figure 1, offers a synthetically efficient route to the subsequent attachment of a redox partner. There were reports of successful light-driven charge separation from BODIPY derivatives to a fullerene electron acceptor attached via the catechol linker.⁵⁻⁸ This was interesting given a prior report of complete quenching of the fluorescence in BODIPY derivatives by the catechol, suggesting efficient excited-state deactivation of the BODIPY by the linker. 9,10 To investigate the general potential for this approach and better understand the underlying dynamics, we recently prepared a series of BODIPY-catechol-fullerene triads. Whereas the parent BODIPY derivatives exhibited large fluorescence quantum yields, no fluorescence was observed from any of the triad assemblies. Despite efficient fluorescence quenching, no compelling evidence of charge transfer to the fullerene was observed. The lack of fluorescence in the BODIPY-catechol dyad precursors led to the hypothesis that the initial photoexcited state on BODIPY-derived chromophores was

rapidly quenched by the catechol linker. This Letter provides strong evidence in support of that hypothesis, quantifies the rate of deactivation, and elucidates the mechanism.

Difluoro- (1x) and catechol-substituted (2x) BODIPY derivatives were prepared, purified, and characterized as described in the Supporting Information (SI). The structures and absorption spectra are presented in Figures 1 and 2, respectively. The 1x compounds all exhibited strong, roughly mirror-image fluorescence with Stokes shifts of 20-40 nm. After the addition of the catechol, there was no measurable fluorescence observed from any of the 2x compounds (Figures S18-S27), indicating a lack of any residual 1x parent compound in the samples and a significant change in the excited-state dynamics. Pump-probe spectroscopy was used to measure the time constants associated with the excited-state dynamics. The pump excitation was set at a wavelength near the absorption maximum for each compound. Complete experimental details, the transient change in optical density, $\Delta OD(\lambda, t)$, at all wavelengths probed, and fits as a function of time for a number of selected probe wavelengths are presented in Figures S56-S80 for all 1x and 2x compounds in Figure 1. All transient spectra for the 1x compounds consisted of a ground-state bleach (GSB, Δ OD < 0), stimulated emission (SE, Δ OD < 0), and excited-state absorption (ESA, Δ OD > 0). The transient spectra appeared within the time resolution

Received: March 15, 2019 Accepted: March 29, 2019 Published: March 29, 2019

1828

Department of Chemistry, University of Minnesota, 207 Pleasant Street Southeast, Minneapolis, Minnesota 55455, United States *Department of Chemistry, University of Manitoba, Winnipeg, Manitoba R3T 2N2, Canada

[§]Department of Chemistry and Biochemistry, University of Minnesota Duluth, 1039 University Drive, Duluth, Minnesota 55812, United States

The Journal of Physical Chemistry Letters

Figure 1. Molecular structures and labels.

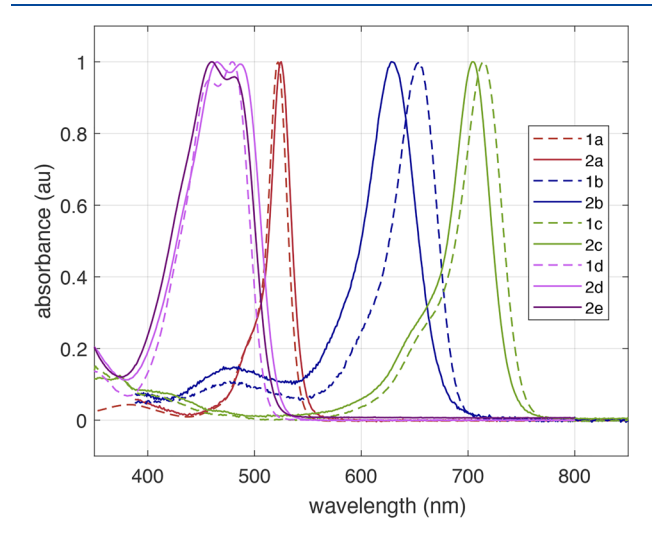


Figure 2. Absorption spectra in toluene for the structures in Figure 1.

of the experiments, \sim 50 fs, did not change shape during the full range of time delays probed, and were well fitted by a first-order decay of the amplitude at all probe wavelengths. The fitted time constants are listed in Table 1 and assigned to the initial optically excited state relaxing directly back to the ground state.

Pump—probe spectra for the 2x compounds differed significantly from those of the 1x precursors. The shape of the spectra changed within the first picosecond, and the transient spectra recovered to the baseline, that is, the original ground state, with time constants that were ca. 1000 times smaller than the analogous 1x compounds. Pump—probe data for 2a are presented in Figure 3. A GSB and SE appeared within the time resolution of the experiment. The negative SE around 580 nm evolved into a positive ESA within the first 100 fs, followed by the subsequent return to the baseline. The data

Table 1. First-Order Time Constants^a

	$ au_{\pi^* o gs}$ (ns)		$ au_{\pi^* o \mathrm{CT}} ext{ (fs)}$	$ au_{\mathrm{CT} o \mathrm{gs}} \; (\mathrm{ps})$
1a	3.1 ± 0.1	2a	100 ± 6	2.9 ± 0.2
1b	1.9 ± 0.1	2b	150 ± 20	4.3 ± 0.9
1c	1.8 ± 0.1	2c	< 500	1.8 ± 0.1
1d	1.8 ± 0.2	2d	<500	15.1 ± 0.5
		2e	< 500	14.0 ± 1.0

 $^a\pi^*$ is the optically excited state, CT is the charge-transfer state, and gs is the electronic ground state.

probed at 580 nm was fitted as two sequential first-order events with time constants of 100 ± 6 fs and 2.9 ± 0.2 ps (Figure 3b). The GSB around 520 nm recovered to the baseline on a comparable time scale to the loss of the intermediate ESA, with a time constant of 3.5 ± 0.3 ps. The data demonstrated very rapid deactivation of the photoexcited state via an intermediate that is accessed on a subpicosecond time scale.

Similar excited-state dynamics were observed for all 2x compounds. Time constants for the two sequential deactivation events are listed in Table 1. The time constants for 2b were determined in the same manner as those for 2a. Evidence of the loss of initial SE and the creation of new ESA features in the first picosecond was present for all 2x compounds; however, the transition from initial photoexcited state to intermediate was not as well resolved at any single point within transient spectra for 2c, 2d, and 2e. An upper limit of 500 fs for the time constant of this first step was determined as a conservative estimate based on the delay time when the overall shape of the transient spectrum stopped changing. The time constants for the second step, return to the ground electronic state, were determined by fits to wavelengths in the probe spectrum dominated by ESA of the intermediate in all cases.

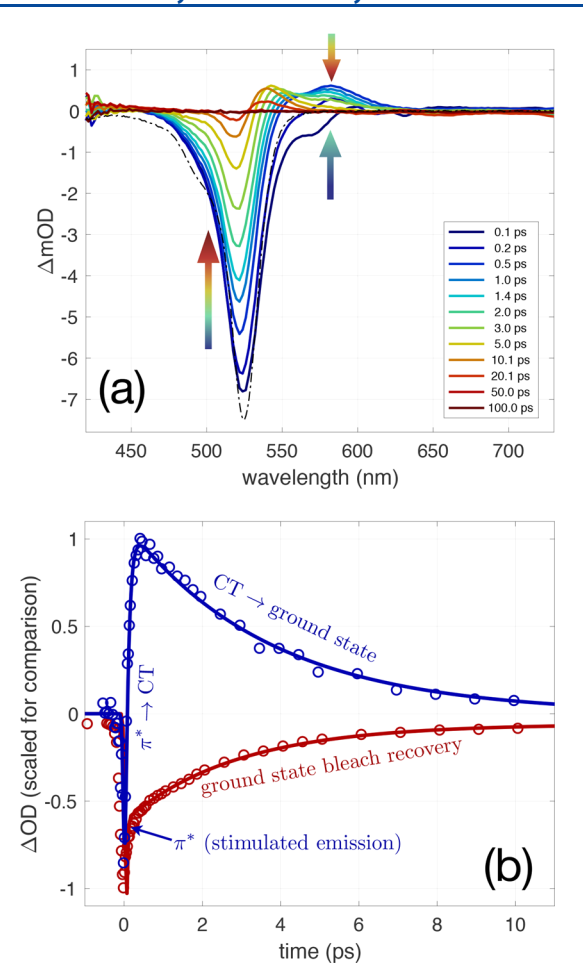


Figure 3. Pump—probe measurements on 2a in toluene excited at 530 nm. (a) Transient change in optical density across the visible spectrum. The black dashed—dotted line is the absorption spectrum inverted and scaled for comparison. (b) Time dependence of the change in optical density at probe wavelengths of 520 (red) and 580 nm (blue). The open circles are the data, and the solid lines are the fits described in the text.

The assignment of the intermediate state responsible for rapid excited-state deactivation was based on computational predictions and measurements of the relative energetics. The top of Figure 4 presents computational predictions for the frontier molecular orbitals using density functional theory (DFT). Complete computational details and associated predictions, including absorption spectra, are available in the SI. The DFT calculations indicated that the HOMO and HOMO-1 were a π orbital on the BODIPY chromophore and an orbital localized on the catechol. These orbitals were reasonably close in energy (<0.5 eV), with the catecholcentered orbital sitting above the π orbital in all cases except 2c. DFT predictions were supported by the spectroscopic and electrochemical measurements presented in Table 2. The last column in Table 2 presents the difference between the optical $\pi \to \pi^*$ gap and the gap between the oxidation of the catechol and the reduction of the π^* orbitals. Measurements indicated orbital energetic alignment of the ground-state π and catechol orbitals, in agreement with the DFT predictions. Experimentally, the orbitals were within 0.4 eV of each other, and the π orbital was lower in energy than the catechol-centered orbital in all cases except 2c. DFT indicated that the initial photoexcitation was dominated by the strongly allowed $\pi \rightarrow$

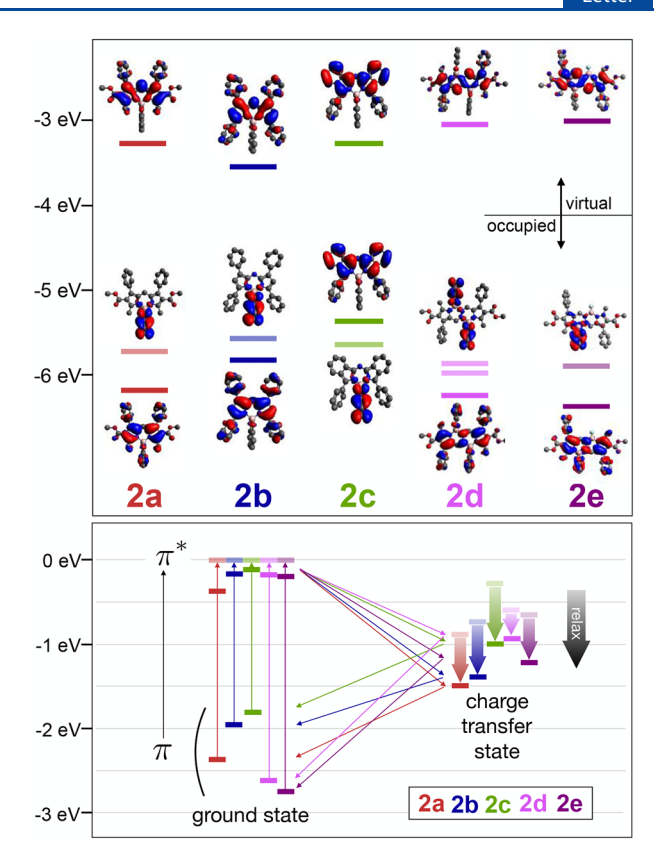


Figure 4. (top) DFT computational predictions for frontier orbital energies. (bottom) TD-DFT computational predictions for energetics relative to the initial optically excited π^* state. Lighter lines represent vertical energies relative to the ground electronic state, and darker lines represent relaxed energies.

Table 2. Energetics^a

	abs max $(\pi \to \pi^*)$	Ox (catechol)	Red (chromophore)	$\Delta_{\pi^* o ext{catechol}}$
2a	2.36	0.86	-1.20	-0.30
2b	1.97	0.74	-0.83	-0.40
2c	1.76	0.81	-1.11	0.16
2d	2.55	0.95	-1.30	-0.30
2e	2.58	0.95	-1.30	-0.33

"All values are in units of electronvolts or volts. Electrochemistry was done in DCM/0.1 M TBAP, and values are relative to the Fc/Fc^+ couple.

 π^* transition, with negligibly small transition dipoles between the π and catechol-centered orbitals. The predicted optically allowed transition and orbital energies suggested a possible mechanism for excited-state deactivation via the transfer of an electron from the catechol to the π orbital on the BODIPY derivative to generate a charge transfer (CT) intermediate state.

Time dependent DFT (TD-DFT) calculations were employed to estimate the relative energetics of the excited π^* and CT states. The calculations included the vertical energy (ground-state geometry) and the optimized (relaxed) excited states in a continuum solvent model with the dielectric constant of toluene (ε = 2.38). The results are presented in the bottom of Figure 4, with the energies referenced to the initial excited π^* state to emphasize the energetic alignment for subsequent dynamics. The CT state is thermodynamically accessible, even prior to the inclusion of relaxation, for all of

state deactivation observed in all cases. A significant fraction of the relaxation in the CT state was attributed to solvation following the increase in the dipole moment. TD-DFT predicted an increase of 2–4.5 D across the series when comparing the ground state to the charge-transfer state. The Kirkwood–Onsager model provides a rough estimate of the differential solvation energy. The solvent polarization energy was expressed in terms of a sphere of radius a in a dielectric continuum of constant ε with a dipole moment μ , $G_P = \frac{\mu^2}{a^3} \left(\frac{2\varepsilon+1}{\varepsilon-1} \right)$. For a sphere of radius 6 Å in a solvent with the dielectric constant of toluene, the difference in the solvent polarization energy for the change in dipole moment predicted for 2a, $8.4 \rightarrow 11.8$ D, is -0.5 eV. This indicates that even in a low dielectric solvent such as toluene, solvation plays a significant role in lowering the energy of the CT state relative to the initially excited state.

the 2x compounds. This is consistent with the rapid excited-

Solvation of the CT state helped facilitate a rapid return to the ground state. Following the relaxation of the CT state, compounds **2a**, **2b**, and **2c** are \sim 1.0 eV above their ground states, whereas compounds **2d** and **2e** are \sim 1.7 eV above their ground states. However, return to the ground state, CT \rightarrow gs, is slower for **2d** and **2e** (Table 1). The reduction in rate with the increase in energy difference and the expectation that reorganization is unlikely to surpass 1.0 eV in toluene lead us to the conclusion that recombination takes place in the Marcus inverted region. Energetic lowering of the CT state through solvation increases the recombination rate, thereby assisting the rapid return to the ground state.

We have demonstrated that a covalently linked catechol is a very efficient excited-state quencher for a series of BODIPYderived chromophores. Following excitation to the optically bright π^* state, subpicosecond conversion to an optically dark CT state, characterized by a shift of electron density from the catechol to the BODIPY-derived chromophore, was followed by rapid return to the ground state in all complexes investigated. These systems covered a broad range of synthetic modification within the BODIPY core, indicating some generality of the excited-state deactivation dynamics in this class of molecules. The results suggest that reports of observed fluorescence in analogous systems may indicate the presence of a residual BODIPY-F2 precursor rather than fluorescence from the BODIPY-catechol dyad. Subpicosecond initial charge separation and the very short lifetime of the penultimate CT state present a substantial hindrance to the successful implementation of the catechol as a linker for the attachment of other redox partners for BODIPY-derived chromophores. This raises significant questions about the previous reports and proposed mechanisms for excited-state charge separation in BODIPY-catechol-fullerene triad sys-

ASSOCIATED CONTENT

S Supporting Information

The Supporting Information is available free of charge on the ACS Publications website at DOI: 10.1021/acs.jp-clett.9b00751.

Experimental details, synthesis, characterization, fluorescence, DFT and TD-DFT calculations, and pump-probe data and fits (PDF)

AUTHOR INFORMATION

Corresponding Authors

*V.N.N.: E-mail: Victor.Nemykin@umanitoba.ca.

*D.A.B.: E-mail: blank@umn.edu.

ORCID 4

Victor N. Nemykin: 0000-0003-4345-0848 David A. Blank: 0000-0003-2582-1537

Note:

The authors declare no competing financial interest.

ACKNOWLEDGMENTS

This work was supported by NSF (DMR-1708177), NSF (CHE-1464711), NSF MRI (MRI-1420373), the Minnesota Supercomputing Institute, NSERC, CFI, University of Manitoba, and WestGrid Canada.

REFERENCES

- (1) Fukuzumi, S.; Ohkubo, K.; Suenobu, T. Long-lived charge separation and applications in artificial photosynthesis. *Acc. Chem. Res.* **2014**, *47*, 1455–1464.
- (2) Hedley, G. J.; Ruseckas, A.; Samuel, I. D. W. Light Harvesting for Organic Photovoltaics. *Chem. Rev.* **2017**, *117*, 796–837.
- (3) Berhe, S. A.; Rodriguez, M. T.; Park, E.; Nesterov, V. N.; Pan, H.; Youngblood, W. J. Optoelectronic tuning of organoborylazadi-pyrromethenes via effective electronegativity at the metalloid center. *Inorg. Chem.* **2014**, *53*, 2346–2348.
- (4) Zatsikha, Y. V.; Maligaspe, E.; Purchel, A. A.; Didukh, N. O.; Wang, Y.; Kovtun, Y. P.; Blank, D. A.; Nemykin, V. N. Tuning Electronic Structure, Redox, and Photophysical Properties in Asymmetric NIR-Absorbing Organometallic BODIPYs. *Inorg. Chem.* **2015**, *54*, 7915–7928.
- (5) Bandi, V.; Das, S. K.; Awuah, S. G.; You, Y.; D'Souza, F. Thienopyrrole-fused 4,4-difluoro-4-bora-3a,4a-diaza-s-indacene-fullerene dyads: Utilization of near-infrared sensitizers for ultrafast charge separation in donor-acceptor systems. *J. Am. Chem. Soc.* **2014**, *136*, 7571–7574.
- (6) Bandi, V.; Gobeze, H. B.; D'Souza, F. Ultrafast Photoinduced Electron Transfer and Charge Stabilization in Donor-Acceptor Dyads Capable of Harvesting Near-Infrared Light. *Chem. Eur. J.* **2015**, *21*, 11483–11494.
- (7) Wijesinghe, C. A.; El-Khouly, M. E.; Blakemore, J. D.; Zandler, M. E.; Fukuzumi, S.; D'Souza, F. Charge stabilization in a closely spaced ferrocene—boron dipyrrin—fullerene triad. *Chem. Commun.* **2010**, *46*, 3301—3303.
- (8) Wijesinghe, C. A.; El-Khouly, M. E.; Subbaiyan, N. K.; Supur, M.; Zandler, M. E.; Ohkubo, K.; Fukuzumi, S.; D'Souza, F. Photochemical charge separation in closely positioned donor-boron dipyrrin-fullerene triads. *Chem. Eur. J.* **2011**, *17*, 3147–3156.
- (9) Shaban Ragab, S.; Swaminathan, S.; Deniz, E.; Captain, B.; Raymo, F. M. Fluorescence Photoactivation by Ligand Exchange around the Boron Center of a BODIPY Chromophore. *Org. Lett.* **2013**, *15*, 3154–3157.
- (10) Tahtaoui, C.; Thomas, C.; Rohmer, F.; Klotz, P.; Duportail, G.; Mély, Y.; Bonnet, D.; Hibert, M. Convenient method to access new 4,4-dialkoxy- and 4,4-diaryloxy-diaza-s-indacene dyes: Synthesis and spectroscopic evaluation. *J. Org. Chem.* **2007**, *72*, 269–272.
- (11) Zatsikha, Y. V.; Swedin, R. K.; Healy, A. T.; Goff, P. C.; Didukh, N. O.; Blesener, T. S.; Kayser, M.; Kovtun, Y. P.; Blank, D. A.; Nemykin, V. N. Synthesis, Characterization, and Electron-Transfer Properties of Ferrocene—BODIPY—Fullerene NIR Absorbing Triads: Are Catecholopyrrolidine-Linked Fullerenes a Good Architecture to Facilitate Electron-Transfer? *Chem.—Eur. J.* 2019, submitted.
- (12) Cramer, C. J. Essentials of Computational Chemistry: Theories and Models, 2nd ed.; John Wiley and Sons, 2004.

- (13) Kirkwood, J. G. Theory of Solutions of Molecules Containing Widely Separated Charges with Special Application to Zwitterions. *J. Chem. Phys.* **1934**, *2*, 351–361.

 (14) Onsager, L. Electric Moments of Molecules in Liquids. *J. Am.*
- Chem. Soc. 1936, 58, 1486-1493.